Thermal suppression of bubble nucleation at first-order phase transitions in the early Universe

Al Ajmi, Mudhahir

2022-07-11

Al Ajmi , M & Hindmarsh , M 2022 , ' Thermal suppression of bubble nucleation at first-order phase transitions in the early Universe ' , Physical Review D , vol. 106 , no. 2 . https://doi.org/10.1103/PhysRevD.106

http://hdl.handle.net/10138/355903
https://doi.org/10.1103/PhysRevD.106.023505

unspecified
publishedVersion

Thermal suppression of bubble nucleation at first-order phase transitions in the early Universe

Mudhahir Al Ajmi[1,*] and Mark Hindmarsh[2,3,†]

[1]*Department of Physics, College of Science, Sultan Qaboos University, P.O. Box 36, P.C. 123, Muscat, Sultanate of Oman*

[2]*Department of Physics and Helsinki Institute of Physics, PL 64, FI-00014 University of Helsinki, Finland*

[3]*Department of Physics and Astronomy, University of Sussex, Falmer, Brighton BN1 9QH, United Kingdom*

(Received 19 May 2022; accepted 23 June 2022; published 11 July 2022)

One of the key observables in a gravitational wave power spectrum from a first order phase transition in the early Universe is the mean bubble spacing, which depends on the rate of nucleation of bubbles of the stable phase, as well as the bubble wall speed. When the bubbles expand as deflagrations, it is expected that the heating of the fluid in front of the phase boundary suppresses the nucleation rate. We quantify the effect, showing that it increases the mean bubble separation, and acts to enhance the gravitational wave signal by a factor of up to order 10. The effect is largest for small wall speeds and strong transitions.

DOI: 10.1103/PhysRevD.106.023505

I. INTRODUCTION

An early Universe cosmological first-order phase transition [1] can lead to interesting physical consequences such as matter-antimatter asymmetry [2], primordial magnetic fields [3,4] and the production of a stochastic background of gravitational waves [5,6] The power spectrum of the gravitational waves contains information about the thermodynamic and transport properties of the system at the time of the phase transition. If the transition happened at around the electroweak scale of 100 GeV, when the Universe was about 10^{-11} seconds old, the gravitational waves could be observable at planned space-based detectors like Laser Interferometer Space Antenna (LISA) [7,8], and the principal thermodynamic and transport properties could be measured over a wide region of the parameter space [9].

The transformation of the metastable phase into the stable one is described by cosmological homogeneous nucleation theory [1,10] (see [11] for a review). Once the temperature has fallen below the critical temperature of the transition T_c, quantum or thermal fluctuations produce small spherical bubbles of the stable phase, which expand and merge, and eventually the whole Universe is converted to its stable phase. The peak of the bubble nucleation rate defines the nucleation temperature T_n, and the time taken to complete the transition can be expressed as a transition rate β. Part of the potential energy of the supercooled metastable phase is converted into bulk fluid motion, which sources gravitational waves long after the transition is completed [12]. The kinetic energy of the bulk fluid motion is controlled by a fourth parameter α, which is essentially the ratio of the potential energy difference to the thermal energy. It quantifies the strength of the transition. The kinetic energy of the bulk motion is also controlled by the equation of state of the fluid, most importantly through the speeds of sound in the two phases [13]. All quantities will be defined more precisely below.

At the end of the transition, the density of bubble nucleation sites n_* defines a mean bubble spacing $R_* = 1/n_*^{1/3}$. If bubble nucleation continues undisturbed in the metastable phase, and the bubbles expand at a constant speed v_w, the mean bubble spacing is given by

$$R_* = (8\pi)^{1/3} v_w/\beta. \tag{1}$$

However, if the bubbles expand as deflagrations [1,14–17], the fluid ahead of the advancing bubble wall is heated, out to the radius of a shock. In this region the nucleation rate is reduced. Thus we expect fewer bubbles to be nucleated, and the mean bubble spacing should increase. The effect acts to increase the peak wavelength of the gravitational wave power spectrum [18,19]. and also the peak power, which scales as R_* or R_*^2, depending on the strength of the transition [8].

The suppression of nucleation by the heating effect has been noted before [20], where it was estimated that nucleation was suppressed everywhere between the wall and the shock. In this paper we quantify the effect more precisely, for transitions with strength parameters up to $\alpha \simeq 1$. We find that the increase in the mean bubble spacing can increase the gravitational wave power by a factor of up

*mudhahir@squ.edu.om
†mark.hindmarsh@helsinki.fi

to O(10), partially compensating the suppression due to the interactions between bubbles [21].

II. BUBBLE NUCLEATION: STANDARD CALCULATION

First, we discuss the formation of bubbles in the plasma according to the standard treatment. We will suppose that the transition rate is much faster than the Hubble rate H, so that we can neglect cosmic expansion. The bubble nucleation rate per unit volume has the form [10,17,22,23]

$$p(t) = p_0 e^{-S(T(t))}. \tag{2}$$

where S is the action for the appearance of a bubble, which in a thermal transition is equal to the energy of a critical bubble divided by the temperature. It is a function of time through its dependence on the temperature $T(t)$. In the small supercooling or "thin wall" approximation [10,23],

$$S \simeq \frac{s_0}{|(1-\hat{T})]^2}, \tag{3}$$

where $\hat{T} = T/T_c$, T_c is the critical temperature, and s_0 is a constant computable from the effective potential of the theory. The nucleation rate is then zero precisely at the critical temperature, and increases very rapidly below it.

Once a bubble has nucleated, it grows at a constant speed v_w, determined by the friction between the wall and the plasma. The increasing population of growing bubbles reduces the fraction of the Universe in the metastable phase.

Let V be the volume in the metastable phase, and V_s the volume in the stable phase, out of a total volume V_{tot}, such that

$$V_{tot} = V + V_s.$$

In the notation of Ref. [23],

$$h = V/V_{tot} \tag{4}$$

denotes the fraction of the Universe in the metastable (high-temperature) phase. First, we consider the reduction in the volume of the unbroken phase between times t and $t + dt$ due to the growth of bubbles nucleated between earlier times t' and $t' + dt'$:

$$d^2V(t,t') = -dN_b(t')4\pi R^2 dR \frac{V(t)}{V(t')}, \tag{5}$$

where dN_b is the number of bubbles nucleated in that time interval, and R is the radius of those bubbles at time t. The factor $V(t)/V(t')$ takes into account the fact that only parts of the bubbles growing into the unbroken phase will change the volume of that phase.

The number of bubbles nucleated between t' and $t' + dt'$ is

$$dN_b = p(t')V(t')dt', \tag{6}$$

where $p(t')$ is the bubble nucleation rate per unit volume, and the factor $V(t')$ accounts for the fact that bubbles nucleate only in the metastable phase. Finally, we have

$$R = v_w(t-t'), \qquad dR = v_w dt, \tag{7}$$

as the bubbles are assumed to grow with constant speed after nucleation.

The nucleation probability is non-zero only below the critical temperature T_c, which is reached at time t_c, so the change in the volume of the stable phase between t and $t + dt$ is, in total,

$$dV(t) = -v_w V(t)dt \int_{t_c}^{t} dt' p(t') 4\pi v_w^2 (t-t')^2. \tag{8}$$

Dividing by the total volume V_{tot}, we obtain a differential equation for h, the fraction remaining in the metastable phase:

$$\frac{dh}{dt} = -v_w h(t) \int_{t_c}^{t} dt' p(t') 4\pi v_w^2 (t-t')^2. \tag{9}$$

It is straightforward to check that the solution to this equation, with the boundary condition $h(t) = 1$ for $t < t_c$, is

$$h(t) = \exp\left(-\frac{4\pi}{3}\int_{t_c}^{t} dt' p(t') v_w^3 (t-t')^3\right). \tag{10}$$

A saddle-point approximation to the integral is possible. We define the transition rate parameter

$$\beta = \frac{d}{dt} \ln p(t)\Big|_{t_f}, \tag{11}$$

where t_f will be specified later, and write

$$p(t) \simeq p_f e^{\beta(t-t_f)} \tag{12}$$

where $p_f = p_0 \exp(-S(t_f))$. The integral can be performed in the approximation $\beta(t_c - t_f) \to -\infty$, giving

$$h(t) = \exp\left(-8\pi v_w^3 \beta^{-4} p_f e^{\beta t}\right). \tag{13}$$

Choosing t_f to be the time at which $h(t_f) = 1/e$, we have

$$h(t) = \exp\left(-e^{\beta(t-t_f)}\right). \tag{14}$$

with

$$8\pi v_w^3 \beta^{-4} p_f = 1. \tag{15}$$

The time t_f is then found as the solution to

$$8\pi v_w^3 \beta^{-4} p_0 e^{-S(t_f)} = 1. \tag{16}$$

Its value does not play an essential role in the following.

To calculate the number of bubbles, we integrate the equation

$$\frac{dN_b}{dt'} = p(t')V(t'), \tag{17}$$

or, in terms of the bubble density $n_b = N_b/V_{tot}$,

$$\frac{dn_b}{dt'} = p(t')h(t'). \tag{18}$$

The final bubble density is then

$$n_b = \beta^3/8\pi v_w^3. \tag{19}$$

We define a mean bubble center spacing R_* as

$$R_* = n_b^{-1/3} = (8\pi)^{1/3}(v_w/\beta). \tag{20}$$

Note that we have assumed that the bubble nucleation rate is the same everywhere in the metastable phase. However, the expanding bubble releases energy and heats up the fluid, as well as setting it in motion. If this heating effect extends in front of the bubble wall, as it does for deflagrations, we can see from (3) that the nucleation rate will be reduced.[1] In the next section we review the calculation the temperature profile around an expanding bubble.

III. HYDRODYNAMICS OF BUBBLE GROWTH BY DEFLAGRATIONS

In order to calculate the suppression effect noted in the previous section, we need to calculate the temperature profile around an expanding bubble for deflagrations.

In the case of perfect fluid the plasma is locally in equilibrium. Therefore, the energy momentum tensor of the fluid can be written as:

$$T^f_{\mu\nu} = w u_\mu u_\nu - g_{\mu\nu} p, \tag{21}$$

where w is the enthalpy density and p is the pressure. The four-velocity field of the plasma u^μ is related to its three-velocity $\mathbf{v}$ by

$$u^\mu = \frac{(1, \mathbf{v})}{\sqrt{1-\mathbf{v}^2}} = (\gamma, \gamma\mathbf{v}). \tag{22}$$

[1]Temperature fluctuations from other sources can also change the nucleation rate [24].

The energy density, e, the enthalpy density w, the entropy density s are related to the pressure as follows:

$$e \equiv T\frac{\partial p}{\partial T} - p, \qquad w \equiv T\frac{\partial p}{\partial T}, \qquad s \equiv \frac{\partial p}{\partial T}. \tag{23}$$

Evidently, $w = e + p$. The motion of the fluid is governed by conservation of energy-momentum:

$$\partial^\mu T^f_{\mu\nu} = 0. \tag{24}$$

The fluid around an expanding spherical bubble at time since nucleation Δt and radial distance r can be described by the purely radial fluid 3-velocity $v(r, \Delta t)$ and enthalpy $w(r, \Delta t)$. The partial differential equations can be solved numerically [15], and it is observed that the fluid quickly settles down to a self-similar solution, depending only on a coordinate $\xi = r/\Delta t$. In this self-similar form, the fluid equations become

$$\frac{dv}{d\xi} = \frac{2v(1-v^2)}{\xi(1-\xi v)}\left(\frac{\mu^2}{c_s^2} - 1\right)^{-1}, \tag{25}$$

$$\frac{dw}{d\xi} = w\left(1 + \frac{1}{c_s^2}\right)\gamma^2\mu\frac{dv}{d\xi}. \tag{26}$$

Here, $c_s^2 = dp/de$ is the speed of sound and

$$\mu = \frac{\xi - v}{1 - \xi v}. \tag{27}$$

is the fluid velocity at ξ in a frame that is moving outward at speed ξ.

We now discuss the boundary conditions at the bubble wall. The plasma is in the stable phase behind the wall, and in the metastable phase in front. We denote quantities evaluated just behind the wall with a subscript $-$, and in front with a subscript $+$, and quantities in the frame moving with the wall with a tilde.

In the frame moving with the wall, conservation of energy density and momentum density imply

$$w_+\tilde{\gamma}_+^2 + p_+ = w_-\tilde{\gamma}_-^2 + p_-, \tag{28}$$

$$w_+\tilde{\gamma}_+^2\tilde{v}_+ = w_-\tilde{\gamma}_-^2\tilde{v}_-, \tag{29}$$

These equations may be rearranged to give

$$\tilde{v}_+ = \frac{1}{1+\alpha_+}\left[\left(\frac{\tilde{v}_-}{2} + \frac{1}{6\tilde{v}_-}\right) \pm \sqrt{\left(\frac{\tilde{v}_-}{2} + \frac{1}{6\tilde{v}_-}\right)^2 + \alpha_+^2 + \frac{2}{3}\alpha_+ - \frac{1}{3}}\right], \tag{30}$$

where

$$\alpha_+ = \frac{4}{3}\frac{\theta_+ - \theta_-}{w_+}, \tag{31}$$

and $\theta = (e - 3p)/4$. In a deflagration, the fluid exits from the wall with the smaller of the wall speed and the sound speed in the stable phase,

$$\tilde{v}_- = \min(v_w, c_s(T_-)). \tag{32}$$

These equations can be straightforwardly solved numerically, once the speed of sound is known as a function of enthalpy density. In practice one wishes to apply the boundary condition at large radii, where $v = 0$ and $T = T_n$, the bubble nucleation temperature. This means that one must "shoot" for this value from an initial guess for α_+. The amount of energy available to be released by the transition is conveniently parametrized by

$$\alpha_n = \frac{4}{3}\frac{\theta_m(T_n) - \theta_s(T_n)}{w_m(t_n)}, \tag{33}$$

where the subscripts m and s denote quantities evaluated in the metastable and stable phases.

In this paper we use the simplest possible equation of state, the bag model, in which

$$p_m = \epsilon + a_m T^4, \qquad p_s = a_s T^4. \tag{34}$$

In this model $c_s^2 = 1/3$ and $w \propto T^4$.

Figure 1 shows plots of temperature profile variation with respect to ξ for different wall speeds ($\xi = 0.4, 0.7$) and for $\alpha_n = 0.2$. The plots were produced by integrating the Eqs. (25) and (26) in parametric form (see [17]), with 5000 points distributed over the parameter range, and an absolute tolerance of 10^{-6} in the shooting parameter α_+.

The upper plot shows the typical form of a subsonic deflagration and the lower one shows a supersonic deflagration (or hybrid) [25]. In each case there is a region of heated fluid, which is moving radially outward, bounded on the outside by a shock, which moves at a speed v_{sh} calculable from the solution to the fluid equations $v(\xi)$ and energy-momentum conservation (see, e.g., [17]. The resulting equation gives the position of the shock as the solution to the equation

$$v(\xi) = \frac{3\xi^2 - 1}{2\xi}. \tag{35}$$

Between the bubble wall and the shock the bubble nucleation rate will be suppressed.

Figure 2 shows the maximum of the ratio of the temperature difference $\Delta T = T - T_n$ to the nucleation temperature T_n as contour lines in the plane of wall speed v_w and transition strength α_n, for a range of $v_w = 0.01$–0.99 and $\alpha_n = 0.005$–1.0. We also show $\Delta T/T_n$ with blue shading, and use it in later figures to give an qualitative indication of

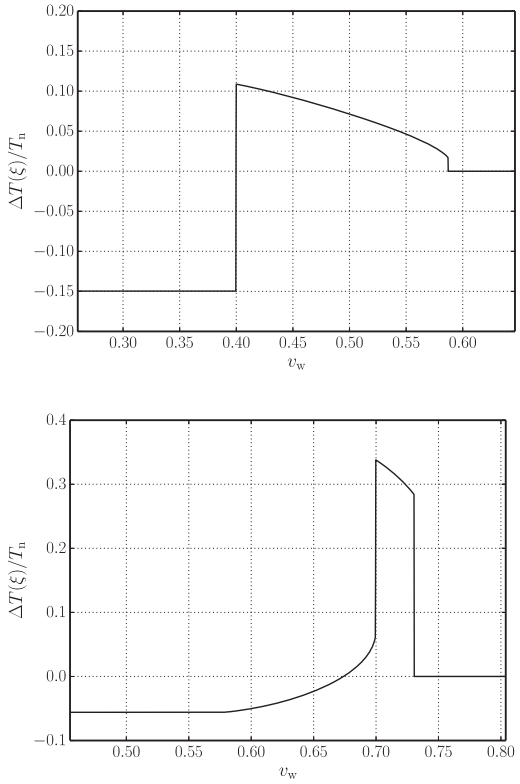

FIG. 1. Variation of temperature with respect to radial similarity variable $\xi = r/t$ in the frame of the bubble center for different wall velocities, $v_w = 0.4$, leading to a deflagration (top) and $v_w = 0.7$ leading to a hybrid (bottom), and phase transition strength parameter $\alpha_n = 0.25$. The plots show the typical profiles for a deflagrations which are subsonic (top) and supersonic (bottom).

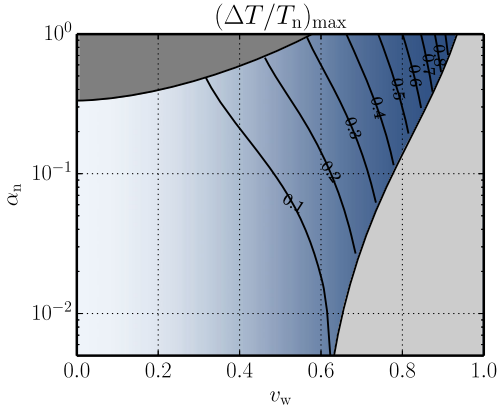

FIG. 2. Contours of the maximum fractional temperature difference around a deflagration, as a function of wall speed v_w and strength parameter at the nucleation temperature α_n. The blue shading also shows the maximum fractional temperature difference, for use in other figures. For larger values of v_w, deflagrations are replaced by detonations and there is no effect. For larger values of α_n, there is no hydrodynamic solution at fixed v_w. Both regions are grayed out.

the accuracy of the calculations, from light (more accurate) to dark blue (less accurate). For large α_n and low v_w there are no solutions to the fluid equations; for large v_w at fixed α_n the solution changes to a detonation, where the wall moves ahead of the shock, and the nucleation suppression effect disappears.

A. Small wall speed limit

In the limit of small wall speed, the fluid velocity should be small ($v(\xi) \ll \xi$), and a simple approximation to the solution to the fluid equations is known. The approximation is

$$v(\xi) = v_{\max} \frac{v_w^2}{\xi^2} \frac{c_s^2 - \xi^2}{c_s^2 - v_w^2}, \tag{36}$$

where $v_{\max}(v_w, \alpha)$ is the maximum fluid speed in the bubble center frame, reached just outside the wall. For small α and v_w not too close to the sound speed [11,16],

$$v_{\max} \simeq 3\alpha_n v_w \frac{1}{1 - 3v_w^2}. \tag{37}$$

This gives an analytic form for the enthalpy,

$$w(\xi) \simeq w_n \exp\left[2(1 + c_s^2) \frac{v_w^2}{c_s^2 - v_w^2} v_{\max} \left(\frac{1}{\xi} - \frac{1}{c_s}\right)\right] \tag{38}$$

where w_n is the enthalpy density at $\xi \geq c_s$, the enthalpy density at the nucleation temperature.

Because $w \propto T^4$, we have for small enthalpy differences $\Delta w/w = 4\Delta T/T$. Hence

$$\begin{aligned} \frac{\Delta T}{T_n} &\simeq \frac{1}{2}(1 + c_s^2) \frac{v_w^2}{c_s^2 - v_w^2} v_{\max} \left(\frac{1}{\xi} - \frac{1}{c_s}\right) \\ &\simeq \frac{3\alpha_n}{2}(1 + c_s^2) \frac{v_w^3}{c_s^2(1 - 3v_w^2)^2} \left(\frac{1}{\xi} - \frac{1}{c_s}\right) \\ &\simeq 6\alpha_n \frac{v_w^3}{(1 - 3v_w^2)^2} \left(\frac{1}{\xi} - \sqrt{3}\right) \end{aligned} \tag{39}$$

This relation is useful in the low velocity region when $v \lesssim 0.05$.

IV. POSITION-DEPENDENT BUBBLE NUCLEATION

In this section, we take into account the dependence of the bubble nucleation rate on the temperature. The temperature is raised closer to the critical temperature in front of a deflagration, and so we expect the nucleation rate to be suppressed around the expanding bubble.

The bubble nucleation rate per unit volume is now space-dependent as well as time dependent, due to the dependence of the bubble appearance action on the temperature:

$$p(t', \mathbf{x}) = p_0 e^{-S(t', \mathbf{x})}. \tag{40}$$

Let us write

$$T(t', \mathbf{x}) = \bar{T}(t') + \Delta T(t', \mathbf{x}), \tag{41}$$

where $\bar{T}$ is the undisturbed temperature outside the shock surrounding each bubble. Hence

$$p(t', \mathbf{x}) = p(t') e^{-\Delta S(t', \mathbf{x})} \tag{42}$$

The rate of bubble nucleation over the remaining volume remaining in the metastable phase $V' \equiv V(t')$ is

$$\frac{dN_b}{dt'} = \int_{V'} d^3x p(t', \mathbf{x}), \tag{43}$$

Hence

$$\frac{dN_b}{dt'} = p(t') \left(V' - \int_{V'} d^3x (1 - e^{-\Delta S})\right), \tag{44}$$

where we have rearranged the equation to bring out a term which acts to reduce the effective volume of the metastable phase. Let us give the correction term the symbol

$$\Delta V_{s,\text{eff}} = \int_{V'} d^3x (1 - e^{-\Delta S}). \tag{45}$$

We can regard this quantity as an increase in the effective volume of the stable phase, where no bubbles can nucleate.

Let us first consider a single bubble nucleated at time t_1, with radius $R = v_w(t' - t_1)$. We can then write

$$\Delta V_{s,\text{eff}} = V_s f, \tag{46}$$

where

$$f = \frac{3}{v_w^3} \int_{v_w}^{v_{sh}} \xi^2 d\xi (1 - e^{-\Delta S}) \tag{47}$$

is a constant factor giving the relative increase in the effective volume of the bubble, v_{sh} is the speed of the shock which surrounds the bubble, and the volume in the stable phase inside the bubble is $V_s = 4\pi v_w^3 (t' - t_1)^3/3$. The effective volume in the stable phase is then

$$V_{s,\text{eff}} = (1 + f) V_s. \tag{48}$$

The change in the bubble appearance action ΔS can be expressed in terms of the transition rate parameter $\beta = -\partial S/\partial t$,

$$\Delta S \simeq \frac{\partial S}{\partial T} \Delta T = \frac{\partial S}{\partial t} \frac{\partial t}{\partial T} \Delta T = \frac{\beta}{H} \frac{\Delta T}{T}. \tag{49}$$

We neglect higher orders in $\Delta T/T$, which means that in the region of (v_w, α_n) plane where $\Delta T/T \sim 1$, our calculations can be expected to receive large corrections. These corrections will depend on the second and higher derivatives of the action with respect to the logarithm of the temperature, parameters which are not part of the standard description of phase transitions. We leave more precise studies for future work, indicating where corrections are likely to be more important by the density of the blue shading in the (v_w, α_n) plane.

With this approximation in mind, we may write

$$f = \frac{3}{v_w^3} \int_{v_w}^{v_{sh}} \xi^2 (1 - e^{-\tilde{\beta}\Delta T(\xi)/T_n}) d\xi \tag{50}$$

where $\tilde{\beta} = \beta/H$, T_n is the nucleation temperature, and $\Delta T(\xi) = T(\xi) - T_n$. We can rewrite the factor in terms of an effective wall speed v_{eff},

$$1 + f = \frac{v_{eff}^3}{v_w^3}. \tag{51}$$

We plot the ratio v_{eff}/v_{sh} on the top row of Fig. 3. We see that for fast ($v_w \gtrsim c_s$) bubble walls in strong ($\alpha_n \gtrsim 0.3$) and rapid ($\tilde{\beta} \gtrsim 100$) transitions, the estimate $v_{eff} \simeq v_{sh}$ is reasonably accurate. However, for slower walls in weak and slow transitions, the approximation fails.

Now let us consider the situation with many bubbles. We label the bubbles by $i = 1, \ldots, N_b$, and define a radial coordinate for each bubble r_i. Before bubbles start overlapping, the effective volume in regions where bubble nucleation has stopped is

$$V_{s,eff} = \sum_{i=1}^{N_b} \frac{4\pi}{3} v_w^3 (t' - t_i)^3 (1 + f) = \sum_{i=1}^{N_b} \frac{4\pi}{3} v_{eff}^3 (t' - t_i)^3. \tag{52}$$

Conversely, the effective volume remaining where bubble nucleation can take place is

$$V_{eff} = V_{tot} - V_{s,eff}. \tag{53}$$

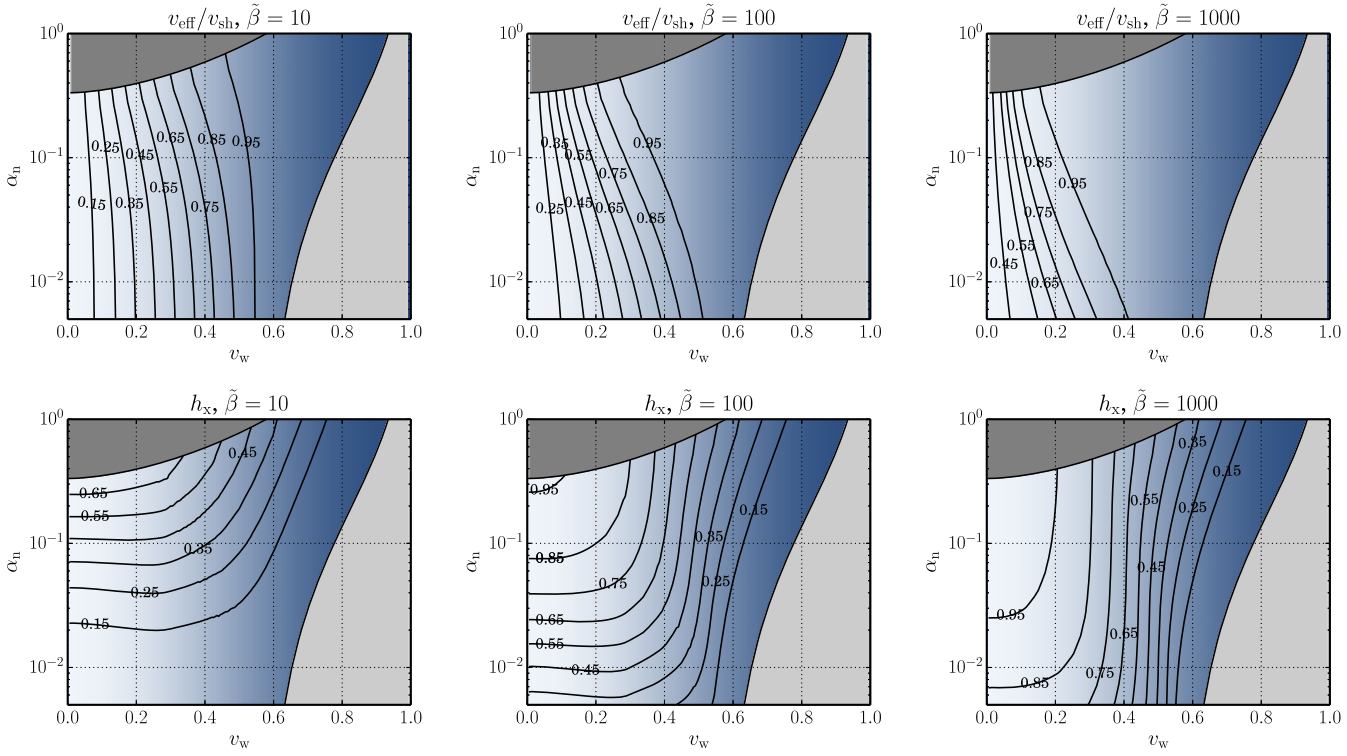

FIG. 3. Top: contour plots of v_{eff}/v_{sh}, where v_{eff} is the expansion speed of the spherical shell inside which further bubble nucleation is effectively suppressed, and v_{sh} is the speed of the shock. For larger β, bubble nucleation is suppressed almost everywhere inside the shock, for a wide range of wall speeds v_w and transition strengths α_n. Bottom: contour plots of h_x, the fractional volume occupied by the metastable phase at which bubble nucleation effectively stops, for values of the transition rate relative to the Hubble rate $\tilde{\beta} = 10$, 100, 1000 (left to right). As $\tilde{\beta}$ increases the effect of nucleation suppression gets larger, due to the increasing sensitivity of the bubble nucleation rate to the temperature. In both rows, the blue shading shows the size of the maximum relative temperature change in the shell, with the same intensity map as in Fig. 2.

The rate of change of the fraction in the metastable phase is then modified to

$$\frac{dh}{dt} = -v_w h \frac{V_{\rm eff}}{V} \int_{t_c}^{t} dt' p(t') 4\pi v_w^2 (t-t')^2. \quad (54)$$

We take the ratio $V_{\rm eff}/V$ to be that from a single bubble,

$$\frac{V_{\rm eff}}{V} = \frac{V_{\rm tot} - V_{\rm s,eff}}{V} \simeq \frac{(1+f)h - f}{h}. \quad (55)$$

This approximation neglects regions outside the shells of radius $v_{\rm eff}(t'-t_i)$ but inside $v_{\rm sh}(t'-t_i)$, where the temperature in overlapping fluid shells has also reached a high enough value to suppress nucleation. This extra volume where nucleation is suppressed will give a small positive correction to $v_{\rm eff}$.

We are also neglecting interactions between the shell of one bubble and the wall of a neighboring one, which tend to slow down the expansion of the wall [21]. We discuss this effect in the conclusions section.

We see that bubbles stop nucleating once h drops below

$$h_x = \frac{f}{1+f} = 1 - \frac{v_w^3}{v_{\rm eff}^3}, \quad (56)$$

so that h_x is the fractional volume at which the symmetric phase is reheated enough to prevent further bubble nucleation. We plot h_x as a function of v_w and α_n, for three values of $\tilde{\beta}$, in the bottom row of Fig. 3.

Hence the equation for the fraction of the universe remaining in the metastable phase h becomes

$$\frac{dh}{dt} = -v_w h(t)(1+f) \int_{t_c}^{t} dt' p(t') \left[1 - \frac{h_x}{h(t')}\right] 4\pi v_w^2 (t-t')^2 \theta(h(t') - h_x), \quad (57)$$

which upon integration with respect to t becomes an integral equation,

$$h(t) = \exp\left(-\frac{4\pi}{3} v_w^3 (1-h_x)^{-1} \int_{t_c}^{t} dt' p(t') \left[1 - \frac{h_x}{h(t')}\right] (t-t')^3 \theta(h-h_x)\right). \quad (58)$$

With the approximation for the nucleation rate per unit volume (12), and defining a dimensionless time variable $\tau = \beta t$, we can rewrite Eq. (58) as

$$h(\tau) = \exp\left[-\frac{1}{6}(1-h_x)^{-1} \int_{\tau_c}^{\tau} d\tau' e^{\tau'-\tau_f} \left(1 - \frac{h_x}{h(\tau')}\right) (\tau-\tau')^3 \theta(h-h_x)\right] \quad (59)$$

where we have used $p_f = \beta^4/8\pi v_w^3$. We see that the equation for h derived in the absence of the suppression effect (9) is recovered in the limit $h_x \to 0$. We assume that $\tau_f - \tau_c \gg 1$, and hence that the solution depends very weakly on τ_c.

We solve this equation for a given h_x by iteration:

$$h^{(a+1)}(\tau) = \exp\left[-\frac{1}{6}(1-h_x)^{-1} \int_{\tau_c}^{\tau} d\tau' e^{\tau'-\tau_f} \left(1 - \frac{h_x}{h^{(a)}(\tau')}\right) (\tau-\tau')^3 \theta(h-h_x)\right] \quad (60)$$

starting with the solution at $f = 0$,

$$h^{(0)}(t) = \exp\left(-e^{\tau'-\tau_f}\right). \quad (61)$$

The iteration converges very quickly and we stop after 5 iterations. The relative difference between the last two iterations depends on h_x and τ but is no greater than 0.01.

For $f \gg 1$, h_x can be close to unity, i.e., bubble nucleation can effectively stop almost immediately. This can happen for large $\tilde{\beta}$.

The fact that the iteration converges very fast motivates a simple approximation,

$$h(\tau) \simeq \begin{cases} h^{(0)}(\tau), & \tau \le \tau_x \\ h^{(1)}(\tau), & \tau > \tau_x \end{cases} \quad (62)$$

Hence, for $\tau > \tau_x$,

$$h(\tau) \simeq \exp\left(-\frac{1}{6}(1-h_{\rm x})^{-1}\int_{\tau_c}^{\tau_{\rm x}} d\tau' e^{\tau'-\tau_f}(1-h_{\rm x}e^{e^{\tau'-\tau_f}})(\tau-\tau')^3\right), \tag{63}$$

The integral can be performed by expanding the exponential (see Appendix), leading to the following equation:

$$h(\tau) \simeq \exp\left(-\frac{e_{\rm x}}{6}(\lambda_0\Delta\tau^3 + 3\lambda_1\Delta\tau^2 + 6\lambda_2\Delta\tau + 6\lambda_3)\right) \tag{64}$$

where $e_{\rm x} \equiv \exp(\tau_{\rm x} - \tau_f)$ and

$$\lambda_a = 1 - \frac{h_{\rm x}}{1-h_{\rm x}}\sum_{m=1}^{\infty}\frac{e_{\rm x}^m}{(m+1)^a} \tag{65}$$

To second order in m,

$$\lambda_a \simeq 1 - \frac{h_{\rm x}}{1-h_{\rm x}}\frac{e_{\rm x}}{2^{a+1}} \tag{66}$$

At this order of approximation, $e_{\rm x}$ can be solved exactly in terms of $h_{\rm x}$ through

$$h(\tau_{\rm x}) \equiv h_{\rm x} = \exp(-e_{\rm x}\lambda_3), \tag{67}$$

leading to the quadratic equation

$$-\frac{h_{\rm x}}{1-h_{\rm x}}\frac{1}{16}e_{\rm x}^2 + e_{\rm x} + \ln h_{\rm x} = 0. \tag{68}$$

For $h_{\rm x} \to 0$ we can neglect $\mathrm{O}(h_{\rm x})$ terms and the solution is $e_{\rm x} = -\ln h_{\rm x}$, with

$$h(\tau) \simeq \exp\left(\frac{1}{6}\ln h_{\rm x}(\Delta\tau^3 + 3\Delta\tau^2 + 6\Delta\tau + 6)\right). \tag{69}$$

For $h_{\rm x} \to 1$, the second terms in the equation for λ_a become important. Writing $h_{\rm x} = 1-\epsilon$, we have

$$e_{\rm x} \simeq \epsilon, \qquad \epsilon \simeq -\ln h_{\rm x}, \qquad \lambda_a \simeq 1 - \frac{1}{2^{a+1}}. \tag{70}$$

Figure 4 shows plots of $h(\tau)$ with different values of $h_{\rm x}$, obtained with the iterative method outlined above. It can be seem that for increasing $h_{\rm x}$, the transition takes longer, as a result of the reduced number density of bubbles nucleated. In the lower panel $\ln(-\ln(h))$ is plotted, along with the approximation derived above.

In the limit $v_{\rm w} \to 0$, the velocity in the fluid shell is small everywhere, and the approximate solution (39) can be used to estimate f. Substituting Eq. (39) in Eq. (50) yields

$$f = \frac{9\alpha\tilde{\beta}}{2c_{\rm s}^2}\frac{(1+c_{\rm s}^2)}{(1-3v_{\rm w}^2)^2}\int_{v_{\rm w}}^{c_{\rm s}}\left(\xi - \frac{\xi^2}{c_{\rm s}}\right)d\xi, \tag{71}$$

$$= \frac{3\alpha\tilde{\beta}}{4c_{\rm s}^2}\frac{(1+c_{\rm s}^2)}{(1-3v_{\rm w}^2)^2}\left(\frac{v_{\rm w}^2(2v_{\rm w}-3c_{\rm s})}{c_s} - c_{\rm s}^2\right) \tag{72}$$

where we have used the fact that the shock speed is approximately $c_{\rm s}$ for deflagrations with low fluid speeds. This expression helps check numerical solutions at low $v_{\rm w}$.

V. DISTANCE BETWEEN BUBBLES

In this section we will derive the equation for the distance between bubbles, for which we need to calculate the bubble number density.

To calculate the number of bubbles, we convert Eq. (44) into an equation the bubble density $n_{\rm b} = N_{\rm b}/V_{\rm tot}$,

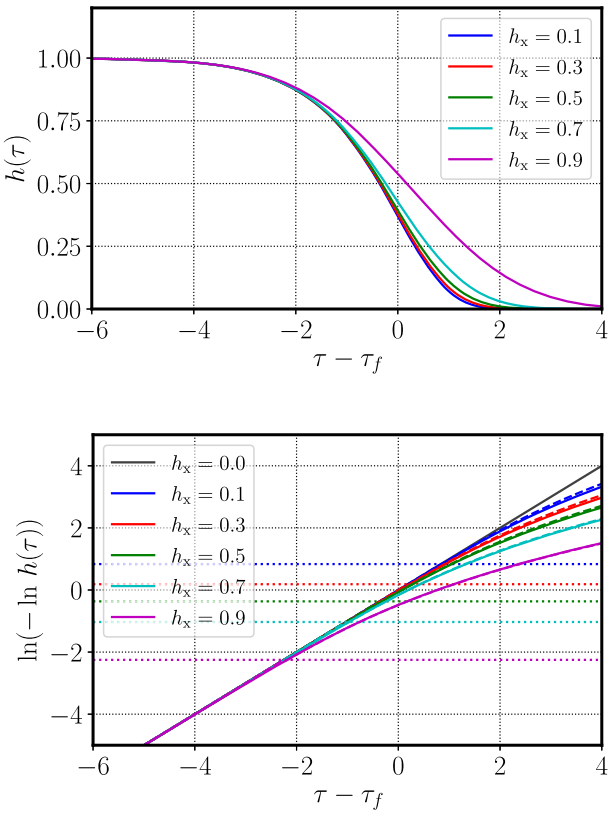

FIG. 4. Plots of $h(\tau)$, where h is the fraction of the universe in the metastable phase, for several values of the threshold fraction where nucleation stops $h_{\rm x}$. Solid lines are the numerical solution to Eq. (63), dashed lines (lower figure) are the approximation Eq. (64). Dotted lines give the threshold values $-\ln h_{\rm x}$.

V. DISTANCE BETWEEN BUBBLES

In this section we will derive the equation for the distance between bubbles, for which we need to calculate the bubble number density.

To calculate the number of bubbles, we convert Eq. (44) into an equation the bubble density $n_{\rm b} = N_{\rm b}/V_{\rm tot}$,

$$\frac{dn_{\rm b}}{dt} = p(t)[(1+f)h(t) - f]. \tag{73}$$

The density of bubbles is, on integrating (73),

$$n_b = \frac{1}{1-h_{\rm x}}\int_{t_c}^{t_{\rm x}} p(t)(h(t)-h_{\rm x})dt, \tag{74}$$

where $t_{\rm x}$ is the time at which nucleation stops, i.e., where $h = h_{\rm x}$.

Introducing the function

$$I_h(h_{\rm x}) = \frac{1}{1-h_{\rm x}}\int_{\tau_c}^{\tau_{\rm x}} e^{\tau-\tau_f}(h(\tau)-h_{\rm x})d\tau \tag{75}$$

we have that

$$n_b(h_{\rm x}) = \beta^{-1}p_f I_h(h_{\rm x}) = n_{\rm b}^{(0)} I_h(h_{\rm x}), \tag{76}$$

where $n_{\rm b}^{(0)} = 8\pi v_{\rm w}^3\beta^3$ is the bubble density in the absence of nucleation suppression. In general, we expect $0 < I_h(h_{\rm x}) < 1$. This function represents the reduction in the mean bubble density by the suppression of the nucleation in advance of the bubbles wall. Clearly, $I_h(0) = 1$. We plot the bubble nucleation rate from the numerical solutions, and the analytic approximation, in Fig. 5.

We recall that the mean bubble center spacing is defined as $R_* = n_{\rm b}^{-1/3}$. Hence, the mean bubble center spacing is increased by a factor

$$\Lambda(h_{\rm x}) \equiv \frac{R_*}{R_*(0)} = I_h^{-1/3}(h_{\rm x}), \tag{77}$$

where $R_*(0) = (8\pi)^{1/3}v_{\rm w}/\beta$ is the mean spacing in the absence of nucleation suppression. Normalized this way, we have $\Lambda(0) = 1$.

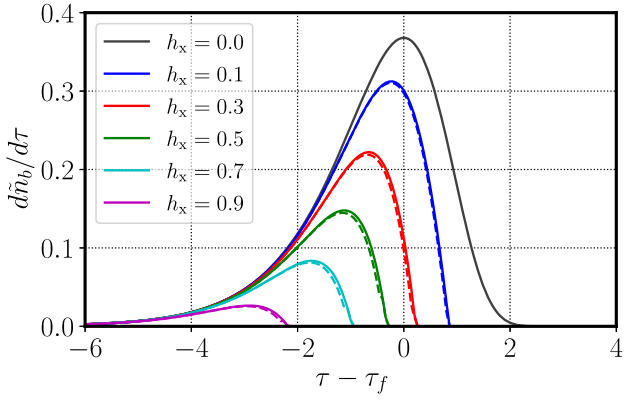

FIG. 5. The universe-averaged dimensionless bubble nucleation rate where $\tilde{n}_b = n_b/n_b^{(0)}$, the rate is given by (73), and the reference bubble density is $n_b^{(0)} = \beta^3/8\pi v_{\rm w}^3$ for the same values of $h_{\rm x}$ as Fig. 4.

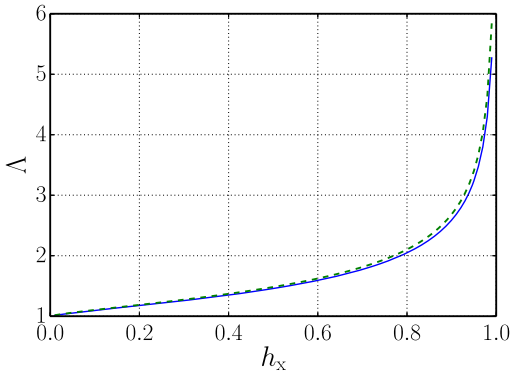

FIG. 6. Bubble spacing enhancement factor Λ as a function of the fractional volume of the universe occupied by the metastable phase at which bubble nucleation stops, $h_{\rm x}$. The blue line uses the numerical solution and the dashed line uses the analytic approximation. As $h_{\rm x} \to 1$, bubble nucleation stops earlier, and the bubbles that are nucleated grow to larger sizes.

The integral can be performed with $h(\tau)$ in its approximate form, leading to

$$I_h(h_{\rm x}) = 1 + \frac{h_{\rm x}\ln h_{\rm x}}{1-h_{\rm x}}. \tag{78}$$

Figure 6 shows the bubble spacing enlargement factor $\Lambda(h_{\rm x})$, computed from the numerical solutions for $h(\tau)$, along with the analytic approximation calculated from (78). As $h_{\rm x}$ increases $\Lambda(h_{\rm x})$ increases demonstrating that

Figure 7 (top row) shows contour plots of $\Lambda(h_{\rm x})$ in the plane of wall speed $v_{\rm w}$ and transition strength parameter $\alpha_{\rm n}$, for $\tilde{\beta} = 10$, 100, 1000. The detonation region and hydrodynamically inaccessible values are grayed out.

VI. GRAVITATIONAL WAVE POWER

The gravitational wave power spectrum produced by a first order phase transition is, in a large region of parameter space, dominated by acoustic production [12,17,19,26] (see also [8,11,27,28] for reviews). The total gravitational wave power is, provided that the mean bubble size is much less than the Hubble length,

$$\Omega_{\rm gw} = 3K^2(v_{\rm w},\alpha)(H_{\rm n}\tau_{\rm v})(H_{\rm n}R_*)\tilde{\Omega}_{\rm gw}, \tag{79}$$

where K is the fraction of the energy of the fluid in the form of kinetic energy, $H_{\rm n}$ is the Hubble rate at nucleation (assumed to be the same as the Hubble rate at the end of the transition), $\tau_{\rm v}$ is the effective lifetime of the source, and $\tilde{\Omega}_{\rm gw} \simeq 10^{-2}$ is a dimensionless parameter characterising the efficiency of gravitational wave production.

The effective source lifetime is the shorter of the Hubble time and the shock appearance timescale $\tau_{\rm sh} = R_*/\sqrt{K}$: once shocks appear, the kinetic energy is dissipated in a time of order a few $\tau_{\rm sh}$. An investigation of how a shear stress source is diluted by expansion [26,29] shows that to a

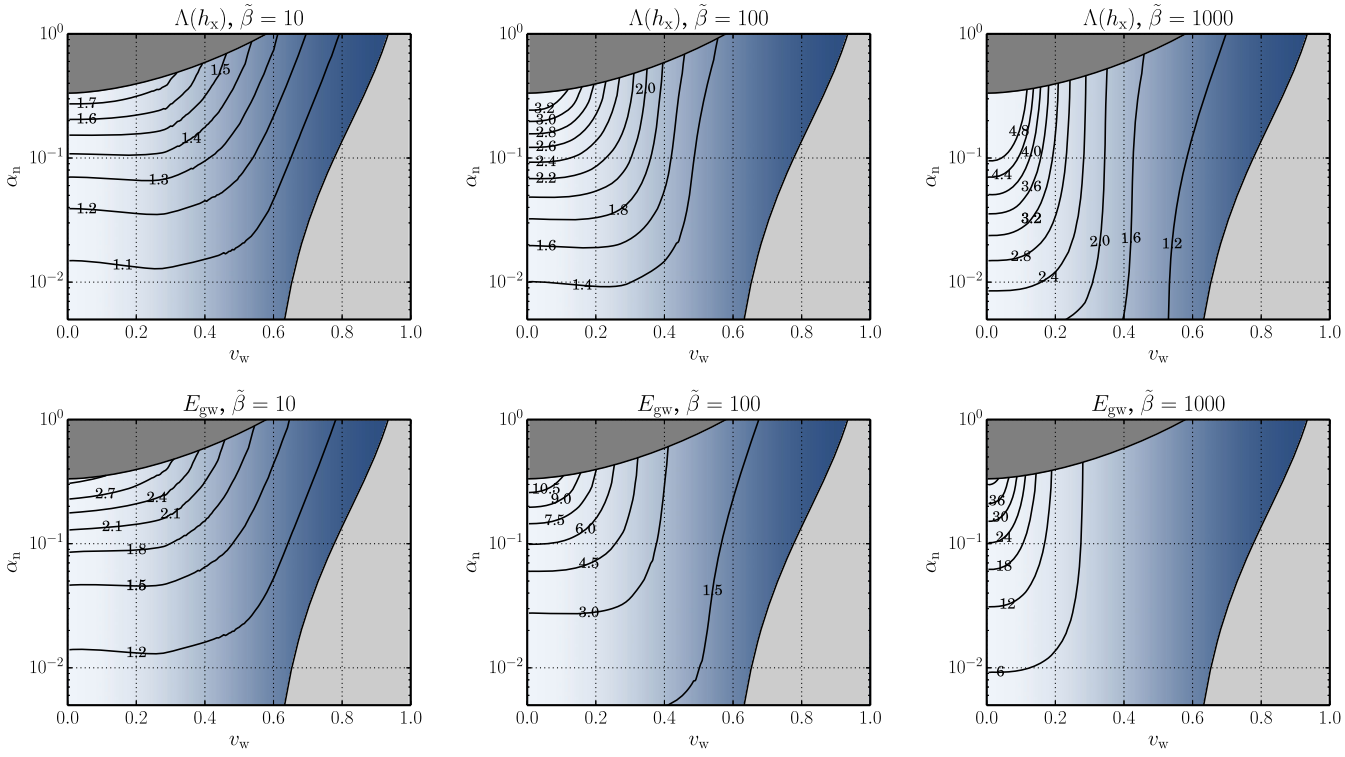

FIG. 7. Top: contour plots of the bubble size enhancement factor Λ ratio in the plane of wall speed v_w and transition strength parameter α_n, for ratios of the transition rate to Hubble rate $\tilde{\beta} = 10$, 100, 1000 (left to right). Contour plots of GW enhancement factor E_{gw} for different temperatures in the plane of α_n and ξ_w. As $\tilde{\beta}$ (the transition rate) increases the E_{gw}) increases. In both rows, the blue shading shows the size of the maximum relative temperature change in the shell, with the same intensity map as in Fig. 2.

first approximation, in which the source is constant and shuts off after time τ_{sh},

$$H_n \tau_v \simeq \left(1 - \frac{1}{\sqrt{1+2x}}\right). \tag{80}$$

For convenience we define

$$J = H_n R_* H_n \tau_v = r_* \left(1 - \frac{1}{\sqrt{1+2x}}\right), \tag{81}$$

where $r_* = H_n R_*$ and $x = r_*/\sqrt{K}$. Recalling the definition of the bubble spacing enhancement factor Λ, the GW power is also enhanced by a factor

$$E_{gw}(v_w, \alpha, \tilde{\beta}) = \Lambda \left(1 - \frac{1}{\sqrt{1 + 2\Lambda r_*(0)/K^{1/2}}}\right). \tag{82}$$

where the Hubble-scaled mean bubble spacing without nucleation suppression is [23]

$$r_*(0) = R_*(0) H_n. \tag{83}$$

In Fig. 7 (bottom row) we show contour plots of the GW enhancement factor E_{gw} for our standard values $\beta/H_n = 10$, 100, 1000. The kinetic energy fraction K has been evaluated using the single-bubble kinetic energy fraction

$$K = \frac{3}{v_w^3 e_n} \int d\xi \xi^2 w \gamma^2 v^2, \tag{84}$$

where v and w are the solution to Eqs. (25), (25), and e_n is the energy density outside the expanding fluid shell. The kinetic energy density is calculated from the numerical solutions, integrated using the trapezium rule.

VII. CONCLUSIONS

In this paper we have studied the suppression of bubble nucleation in cosmological phase transitions proceeding by deflagrations. In a deflagration, some of the energy released by the transition goes into heating up the fluid in front of the bubble wall which, as a result, suppresses further bubble nucleation. In a detonation, on the other hand, the bubble wall is ahead of the shell of excess thermal energy, and the effect is absent.

We find that nucleation stops when a certain fraction of the volume in the metastable phase has been converted. The fraction can easily be computed from the solution of the relativistic hydrodynamic equations, in an expansion in the relative temperature fluctuation $\Delta T/T_n$. We solve the

equations for a fluid with a bag model equation of state, and compute the first order effect. This is sufficient for transition strengths below around 0.3, and wall speeds below the sound speed.

The suppression of nucleation results in a lower number of bubbles per unit volume, and therefore a larger mean distance between their centers. The effect results in a larger intensity of gravitational waves from the transition.

The region of higher temperature extends outward to a leading shock, which travels faster than the sound speed. For this reason it has sometimes been estimated that the region extends out to the shock speed $v_{\rm sh}$ [20] or the sound speed (an estimate of the shock speed) [8]. Here we have shown that the effect is more complicated. The suppression can be expressed as the effective speed $v_{\rm eff}$ of expanding spherical volumes inside which nucleation stops, with $v_{\rm w} < v_{\rm eff} < v_{\rm sh}$. We show that this approximation $v_{\rm eff} \simeq v_{\rm sh}$ works well for fast walls in strong and rapid transitions, but not otherwise.

The more rapid the phase transition, as measured by the parameter $\tilde{\beta}$, the more sensitive the system is to the suppression effect. This is because $\tilde{\beta}$ is equal to the logarithmic derivative of the nucleation probability with respect to the temperature. Increasing the phase transition strength parameter $\alpha_{\rm n}$ also increases the effect, as one would expect from the larger release of thermal energy. The effect also increases with decreasing wall speed $v_{\rm w}$, as the heated volume is larger relative to the bubble size.

For example, for $(v_{\rm w}, \alpha_{\rm n}, \tilde{\beta}) = (0.1, 3 \times 10^{-2}, 1000)$, the ratio $v_{\rm eff}/v_{\rm sh} \simeq 0.4$, and bubbles stop nucleating when only 5% of the universe has been converted to the stable phase. This has the effect of increasing the mean bubble spacing by a factor 4, and the gravitational wave intensity by a factor 5. We show the magnitude of both effects, as functions of $v_{\rm w}$ and $\alpha_{\rm n}$, in contour plots in Fig. 7.

Our results are derived from a numerical solution to an integral equation for the fraction remaining in the metastable phase as a function of time, $h(t)$. We have also shown that good numerical approximations exist, and that the suppression factors can be calculated from the solution of the relativistic hydrodynamic equations.

A further effect to consider for precise calculations of the gravitational wave power spectrum is the altered collision time distribution [17]. In the standard calculation with exponentially growing nucleation rate per unit volume of metastable phase, the distribution of times between a segment of wall being nucleated, and colliding with another segment of wall, is distributed exponentially. If all bubbles are nucleated simultaneously, the distribution is a power times an exponential. As $h_{\rm x}$ is reduced from 1 to 0, we are effectively interpolating between these two situations, and we therefore expect the shape of the gravitational wave power spectrum to interpolate between the exponential and simultaneous [17] as well.

Finally, in this paper we have assumed that the walls expand with a constant speed throughout the transition. On the other hand, when a bubble wall encounters the heated region surrounding another bubble, the pressure difference across it will be reduced, and the wall will slow down [21]. If the nucleation has effectively stopped by the time the bubble walls start to slow, the number of bubbles nucleated per unit volume, and hence the mean bubble spacing R_*, will not be affected. The effect of the walls slowing will therefore be smaller for larger $h_{\rm x}$, and hence larger $\tilde{\beta}$. We therefore expect the slowing of the walls to be important only for lower values of $\tilde{\beta}$. We will explore the effect in more detail elsewhere.

ACKNOWLEDGMENTS

We thank Daniel Cutting, Stephan Huber, Jose-Miguel No, Kari Rummukainen and David Weir for useful comments and discussions. M. A.-A. acknowledges the University of Sussex for hosting him in his sabbatical leave period. He also thanks Sultan Qaboos University for support with Grants No. IG/SCI/PHYS/17/05 and No. IG/SCI/PHYS/20/02. M. H. acknowledges support from the Academy of Finland Grant No. 333609. Computations were performed using NumPy [30] and SciPy [31]. All plots were made with MATPLOTLIB [32].

APPENDIX: DETAILED CALCULATION OF $h_{\rm x}$

We study the integral in the exponent of Eq. (63),

$$L(\tau) = \int_{\tau_c}^{\tau_{\rm x}} d\tau' e^{\tau'-\tau_f}(1 - h_{\rm x} e^{e^{\tau'-\tau_f}})(\tau - \tau')^3. \tag{A1}$$

By expanding the first exponential, and writing $e_{\rm x} \equiv e^{\tau'-\tau_f}$ we have

$$L(\tau) = e^{\tau_{\rm x}-\tau_f} \int_{\tau_c}^{\tau_{\rm x}} d\tau' e^{\tau'-\tau_{\rm x}} \left(1 - h_{\rm x} \sum_{m=0}^{\infty} \frac{e_{\rm x}^m}{m!} e^{m(\tau'-\tau_{\rm x})}\right) \times (\Delta\tau + \tau_{\rm x} - \tau')^3, \tag{A2}$$

where $\Delta\tau = \tau - \tau_{\rm x}$. As the integrals are dominated by their upper limits, it is a good approximation to take $\tau_c \to -\infty$, leading us to consider

$$K_m(\tau) = \int_{-\infty}^{\tau_{\rm x}} d\tau' e^{(m+1)(\tau'-\tau_{\rm x})}(\Delta\tau + \tau_{\rm x} - \tau')^3 = k_m^0 \Delta\tau^3 + 3k_m^1 \Delta\tau^2 + 3k_m^2 \Delta\tau + k_m^3, \tag{A3}$$

where

$$k_m^a = \frac{a!}{(m+1)^a}. \tag{A4}$$

Hence

$$L(\tau) = (1-h_{\rm x})\sum_{m=0}^{\infty} A_m (k_m^0 \Delta\tau^3 + 3k_m^1 \Delta\tau^2 + 3k_m^2 \Delta\tau + k_m^3)$$

where

$$A_m = \begin{cases} 1, & m = 0, \\ -\frac{h_{\rm x}}{1-h_{\rm x}} \frac{e^{m(\tau_{\rm x}-\tau_f)}}{m!}, & m > 0. \end{cases} \tag{A5}$$

Finally, we write

$$h(\tau) \simeq \exp\left(-\frac{e_{\rm x}}{6}(\lambda_0 \Delta\tau^3 + 3\lambda_1 \Delta\tau^2 + 6\lambda_2 \Delta\tau + 6\lambda_3)\right), \tag{A6}$$

where

$$\lambda_a = 1 - \frac{h_{\rm x}}{1-h_{\rm x}} \sum_{m=1}^{\infty} \frac{e_{\rm x}^m}{(m+1)^a}. \tag{A7}$$

[1] P. J. Steinhardt, Phys. Rev. D **25**, 2074 (1982).
[2] V. A. Kuzmin, V. A. Rubakov, and M. E. Shaposhnikov, Phys. Lett. **155B**, 36 (1985).
[3] C. J. Hogan, Phys. Rev. Lett. **51**, 1488 (1983).
[4] G. Baym, D. Bodeker, and L. D. McLerran, Phys. Rev. D **53**, 662 (1996).
[5] E. Witten, Phys. Rev. D **30**, 272 (1984).
[6] C. J. Hogan, Mon. Not. R. Astron. Soc. **218**, 629 (1986).
[7] P. Amaro-Seoane *et al.* (LISA Collaboration), arXiv:1702.00786.
[8] C. Caprini *et al.*, J. Cosmol. Astropart. Phys. 03 (2020) 024.
[9] C. Gowling and M. Hindmarsh, J. Cosmol. Astropart. Phys. 10 (2021) 039.
[10] A. D. Linde, Nucl. Phys. **B216**, 421 (1983).
[11] M. B. Hindmarsh, M. Lüben, J. Lumma, and M. Pauly, SciPost Phys. Lect. Notes **24**, 1 (2021).
[12] M. Hindmarsh, S. J. Huber, K. Rummukainen, and D. J. Weir, Phys. Rev. Lett. **112**, 041301 (2014).
[13] F. Giese, T. Konstandin, K. Schmitz, and J. Van De Vis, J. Cosmol. Astropart. Phys. 01 (2021) 072.
[14] L. D. Landau and E. M. Lifshitz, *Fluid Mechanics*, 2nd ed., Course of Theoretical Physics (Butterworth-Heinemann, 1987), Vol. 6.
[15] H. Kurki-Suonio and M. Laine, Phys. Rev. D **54**, 7163 (1996).
[16] J. R. Espinosa, T. Konstandin, J. M. No, and G. Servant, J. Cosmol. Astropart. Phys. 06 (2010) 028.
[17] M. Hindmarsh and M. Hijazi, J. Cosmol. Astropart. Phys. 12 (2019) 062.
[18] M. Hindmarsh, Phys. Rev. Lett. **120**, 071301 (2018).
[19] M. Hindmarsh, S. J. Huber, K. Rummukainen, and D. J. Weir, Phys. Rev. D **96**, 103520 (2017).
[20] G. D. Moore and K. Rummukainen, Phys. Rev. D **63**, 045002 (2001).
[21] D. Cutting, M. Hindmarsh, and D. J. Weir, Phys. Rev. Lett. **125**, 021302 (2020).
[22] A. H. Guth and E. J. Weinberg, Phys. Rev. D **23**, 876 (1981).
[23] K. Enqvist, J. Ignatius, K. Kajantie, and K. Rummukainen, Phys. Rev. D **45**, 3415 (1992).
[24] R. Jinno, T. Konstandin, H. Rubira, and J. van de Vis, J. Cosmol. Astropart. Phys. 12 (2021) 019.
[25] H. Kurki-Suonio and M. Laine, Phys. Rev. D **51**, 5431 (1995).
[26] M. Hindmarsh, S. J. Huber, K. Rummukainen, and D. J. Weir, Phys. Rev. D **92**, 123009 (2015).
[27] D. J. Weir, Phil. Trans. R. Soc. A **376**, 20170126 (2018).
[28] A. Mazumdar and G. White, Rep. Prog. Phys. **82**, 076901 (2019).
[29] H.-K. Guo, K. Sinha, D. Vagie, and G. White, J. Cosmol. Astropart. Phys. 01 (2021) 001.
[30] C. R. Harris *et al.*, Nature (London) **585**, 357 (2020).
[31] P. Virtanen *et al.*, Nat. Methods **17**, 261 (2020).
[32] J. D. Hunter, Comput. Sci. Eng. **9**, 90 (2007).